The Plant Cell, Vol. 21: 786–799, March 2009, www.plantcell.org

Obligate Heterodimerization of *Arabidopsis* Phytochromes C and E and Interaction with the PIF3 Basic Helix-Loop-Helix Transcription Factor[W]

Ted Clack, Ahmed Shokry, Matt Moffet, Peng Liu, Michael Faul, and Robert A. Sharrock[1]

Department of Plant Sciences and Plant Pathology, Montana State University, Bozeman, Montana 59717

Phytochromes are dimeric chromoproteins that regulate plant responses to red (R) and far-red (FR) light. The *Arabidopsis thaliana* genome encodes five phytochrome apoproteins: type I phyA mediates responses to FR, and type II phyB–phyE mediate shade avoidance and classical R/FR-reversible responses. In this study, we describe the complete in vivo complement of homodimeric and heterodimeric type II phytochromes. Unexpectedly, phyC and phyE do not homodimerize and are present in seedlings only as heterodimers with phyB and phyD. Roles in light regulation of hypocotyl length, leaf area, and flowering time are demonstrated for heterodimeric phytochromes containing phyC or phyE. Heterodimers of phyC and chromophoreless phyB are inactive, indicating that phyC subunits require spectrally intact dimer partners to be active themselves. Consistent with the obligate heterodimerization of phyC and phyE, phyC is made unstable by removal of its phyB binding partner, and overexpression of phyE results in accumulation of phyE monomers. Following a pulse of red light, phyA, phyB, phyC, and phyD interact in vivo with the PHYTOCHROME INTERACTING FACTOR3 basic helix-loop-helix transcription factor, and this interaction is FR reversible. Therefore, most or all of the type I and type II phytochromes, including heterodimeric forms, appear to function through PIF-mediated pathways. These findings link an unanticipated diversity of plant R/FR photoreceptor structures to established phytochrome signaling mechanisms.

INTRODUCTION

Red (R) and far-red (FR) light and the ratio of these colors are key environmental cues in the regulation of plant growth and development, reproduction, circadian rhythms, and competitive responses. Phytochromes (phys) are soluble chromoprotein receptors that exist in two photointerconvertible forms, R-absorbing Pr and FR-absorbing Pfr (Rockwell et al., 2006; Bae and Choi, 2008). The presence of R converts inactive Pr molecules to the signaling-active Pfr conformation, and, conversely, FR converts them back to inactive Pr. Phytochromes are found in eukaryotes, including plants, green algae, and fungi, and in prokaryotes, including both photosynthetic cyanobacteria and eubacteria (Sharrock, 2008). In eukaryotes, the phy Pr and Pfr forms are predominantly cytosolic and nuclear in location, respectively (Nagatani, 2004; Kevei et al., 2007). Moreover, in higher plants, a large number of downstream signaling partner proteins have been shown to bind differentially to these two photoreversible conformers (Castillon et al., 2007; Quail, 2007; Bae and Choi, 2008).

Plants contain multiple forms of phytochrome, and, in angiosperms, these fall into two functional groups, type I and type II. In *Arabidopsis thaliana*, there are five *PHY* genes (*PHYA–PHYE*), and analysis of laboratory mutants, natural sequence variants, and transgenic lines with altered *PHY* gene expression has revealed many of their in vivo functions. Type I phyA is the primary photoreceptor for very low fluence responses to a broad spectrum of light and for high irradiance responses to continuous FR. Type II phyB–phyE principally regulate R/FR photoreversible low fluence responses and shade-avoidance/neighbor-sensing responses to the ratio of R to FR (Mathews, 2006; Rockwell et al., 2006). Plant phys have a conserved domain structure: PLD-GAF-PHY-PAS-PAS-HKRD (Figure 1A), where domain designations are PAS (Per/Arnt/Sim), PLD (PAS-like), GAF (cGMP phosphodiesterase/adenyl cyclase/*Fhl1*), PHY (phytochrome-specific), and HKRD (histidine kinase-related domain). Crystal structures for the chromophore binding/photosensory N-terminal PLD-GAF and PLD-GAF-PHY regions of several prokaryotic phytochromes have been determined (Wagner et al., 2005, 2007; Yang et al., 2007, 2008; Essen et al., 2008). However, the structure of the plant-specific C-terminal PAS-PAS-HKRD region remains to be solved. Evidence has been presented for R-mediated uncovering of a nuclear localization signal located within the phyB PAS-PAS region (Chen et al., 2005). In addition, various types of experiments, including analysis of the behavior of phy fragments expressed in vivo, yeast and bacterial interaction assays, and results of site-directed mutagenesis indicate that phyA and phyB dimerize via sequences in their C-terminal regions (Edgerton and Jones, 1992; Cherry et al., 1993; Wagner et al., 1996; Kim et al., 2006).

Homodimers of phyA and phyB have been observed in wild-type and phy overexpresser lines (Jones and Quail, 1986; Wagner et al., 1996), and the native complement of

[1] Address correspondence to sharrock@montana.edu.
The author responsible for distribution of materials integral to the findings presented in this article in accordance with the policy described in the Instructions for Authors (www.plantcell.org) is: Robert A. Sharrock (sharrock@montana.edu).
[W]Online version contains Web-only data.
www.plantcell.org/cgi/doi/10.1105/tpc.108.065227

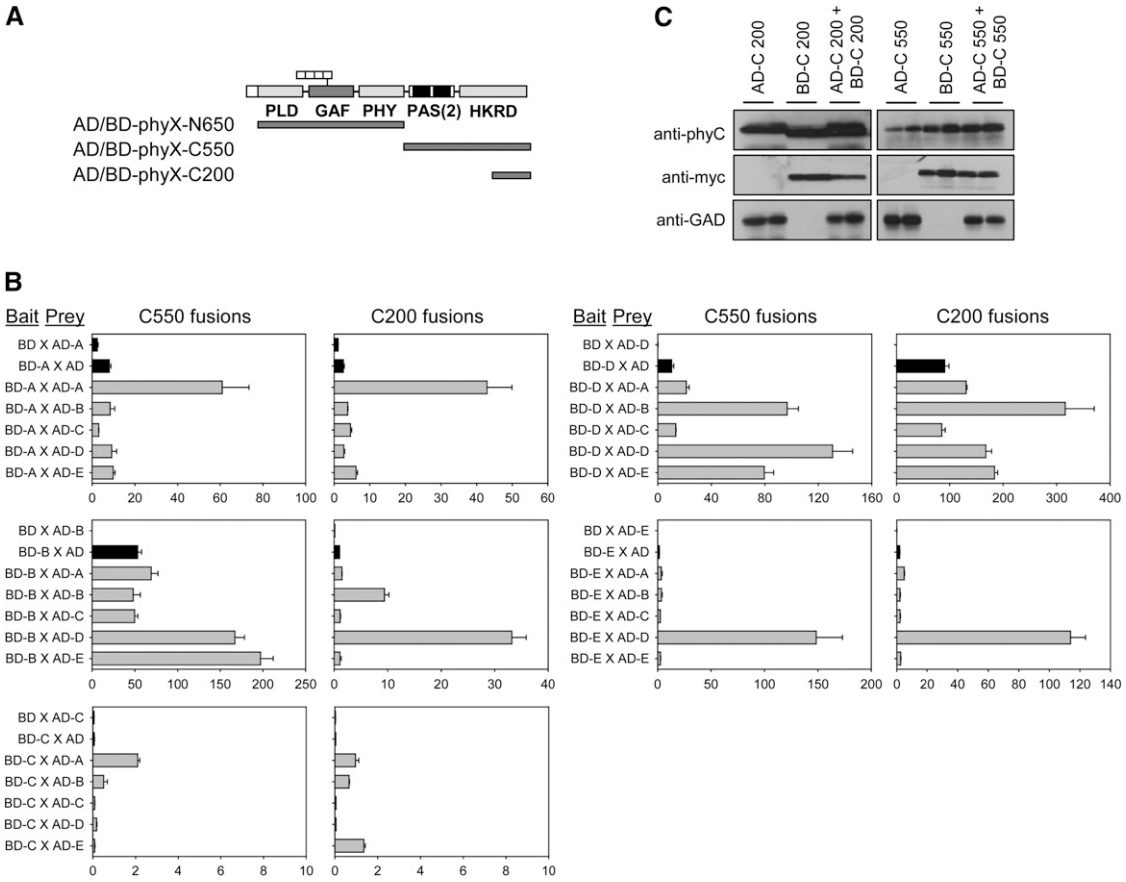

Figure 1. Yeast Two-hybrid Analysis of Binding Interactions among the Five *Arabidopsis* Phytochrome C Termini.

(A) Illustration of the protein domains common to plant phytochromes and the regions of the phytochrome apoproteins used in yeast two-hybrid experiments. The chromophore attachment site within the GAF domain is indicated. Phytochrome domains are PAS (Per/Arnt/Sim), PLD (PAS-like), GAF (cGMP phosphodiesterase/adenyl cyclase/*Fhl1*), PHY (phytochrome-specific), and HKRD (histidine kinase-related domain). The indicated N-terminal or C-terminal phytochrome sequences were fused to the GAL4 AD and DNA BD.

(B) Liquid β-galactosidase assay activities for all pairwise combinations of the C-terminal sequences of phyA through phyE. The amino acid sequence coordinates for the individual C-550 and C-200 regions are given in Methods. Error bars represent the SE from three replicate experiments. Note the scale for the phyC panels is at background levels.

(C) Immunoblot analysis of yeast strains expressing the phyC C-terminal fusions. Proteins were extracted from yeast strains expressing the phyC-C200 and phyC-C550 fusions. Extracts were separated by SDS-PAGE, blotted, and probed with anti-myc, anti-GAD, and anti-phyC antibodies.

phytochromes in plants has often been assumed to consist of only homodimeric forms. However, in *Arabidopsis*, heterodimers of type II phys have been observed in vivo (Sharrock and Clack, 2004). Formation of such heteromeric photoreceptors increases the potential complexity of R/FR light sensing and signaling mechanisms in plants. Analysis of *phyB* mutants has shown that this phy has a very prominent role in R/FR ratio-sensing and R/FR-reversible responses (Somers et al., 1991; Reed et al., 1993; Weller et al., 1995; Takano et al., 2005). By contrast, *phyC*, *phyD*, and *phyE* mutants in *Arabidopsis* and *phyC* mutants in rice (*Oryza sativa*) are only mildly deficient in R/FR sensitivity compared with the wild type (Aukerman et al., 1997; Devlin et al., 1998; Franklin et al., 2003a; Monte et al., 2003; Takano et al., 2005), indicating that these phy forms mediate more subtle shade/neighbor-induced or R/FR-reversible responses, fine-tuning light development in concert with phyB. This can readily be reconciled with the origin of phyD as the product of a recent duplication of the *PHYB* gene in *Brassicaceae* (Mathews and McBreen, 2008). However, the *PHYC* and *PHYE* genes are ancient and widely distributed in flowering plants (Mathews and Sharrock, 1997; Mathews, 2006), particularly *PHYC*, which arose before the origin of angiosperms, and the in vivo mechanisms of their subtle individual activities and their interactions with phyB are not known.

Phytochromes A and B bind to a large number of signaling proteins in an R/FR light-dependent manner (Castillon et al., 2007; Quail, 2007; Bae and Choi, 2008). The PIF1/PIL5, PIF3, PIF4, PIF5/PIL6, PIF6/PIL2, and PIF7 basic helix-loop-helix (bHLH) proteins are principally negative regulators of photomorphogenesis, bind preferentially to the Pfr form of one or both of these phytochromes in vitro, and in most cases are degraded in vivo in phy-dependent ways after transfer from the dark to R (Ni

et al., 1998, 1999; Zhu et al., 2000; Huq and Quail, 2002; Khanna et al., 2004; Oh et al., 2004; Al-Sady et al., 2006; Leivar et al., 2008). The Pfr forms of phyA, phyB, and phyD transiently colocalize with PHYTOCHROME INTERACTING FACTOR3 (PIF3) in nuclear bodies that form within 2 min of exposure to FR or R light (Bauer et al., 2004). This R-induced association with nuclear bodies and the phosphorylation and degradation of PIF3 in vivo are dependent upon the presence of at least one of either the active phyA binding or the active phyB binding (APB) domains of PIF3 (Al-Sady et al., 2006). PIF1 has been shown to interact with both phyA and phyB in vivo (Shen et al., 2008). However, conformation-dependent interactions between phys and most of the PIFs, including PIF3, have not been confirmed by pull-down assays from plant extracts. Moreover, phyC, phyD, and phyE do not bind to the APB domain of PIF3 protein in vitro as Pr or Pfr, suggesting that these phytochromes may signal through other pathways (Khanna et al., 2004).

In this study, we have characterized the dimerization specificities of the *Arabidopsis* phytochromes in yeast two-hybrid analyses and by coimmunoprecipitation (co-IP) from seedling extracts. We find that two phytochrome forms, phyC and phyE, do not homodimerize and, instead, heterodimerize with phyB and phyD. Since the *PHYC* gene evolved very early and representatives of this gene lineage are found in most angiosperms (Mathews and Sharrock, 1997; Mathews, 2006), heterodimerization is likely a fundamental property of phytochromes throughout plants. In addition, we show that phyA, phyB, phyC, and phyD coimmunoprecipitate from seedling extracts with the PIF3 transcription factor in a R/FR-reversible manner. Hence, most or all phytochromes, including heterodimeric forms, appear to function through PIF-mediated pathways.

RESULTS

Phytochrome C-Terminal Binding Interactions

Yeast two-hybrid assays were performed with the *Arabidopsis* phyA through phyE N-terminal chromophore binding/photosensory regions and with large and small fragments of the C-terminal regions as shown in Figure 1A. No interaction was detected among the 600– to 650–amino acid N-terminal regions, which is consistent with previous observation that the truncated N-terminal regions of phyA and phyB remain monomeric when expressed in plants (Cherry et al., 1993; Wagner et al., 1996). The large C-550 PAS-PAS-HKRD phy regions and the small C-200 phy regions exhibit distinctive patterns of self- and cross-interaction. Figure 1B shows β-galactosidase assay results for all combinations of these C-terminal regions. In control assays, while all of the phy C-550 and C-200 fusions to the GAL4 activation domain (AD) have very low background activities by themselves, several of the GAL4 DNA binding domain (BD) fusions show autoactivation of β-galactosidase, notably the BD-phyB-C550 and BD-phyD-C200 constructs. Taking these background values into account, assay results indicate that the following binding interactions are mediated by sequences in both the phytochrome C550 and C200 clones: A/A, D/D, B/D, B/E, and D/E. Interaction between the phyB and phyE C termini is seen in the AD-phyE-C550 X BD-phyB-C550 assay but not in the reciprocal assay or in assays using the C200 regions of these apoproteins (Figure 1B). The β-galactosidase enzyme values for homodimerization of phyB are low and are seen only with the C200 region. Nevertheless, these assays are consistent with all of the heterodimerization interactions previously observed (Sharrock and Clack, 2004) and with observations that homodimerization of both phyA and phyB is mediated by sequences in their PAS domains and C-terminal 200 amino acids (Edgerton and Jones, 1992; Cherry et al., 1993; Wagner et al., 1996; Kim et al., 2006).

Although the C-200 and C-550 AD-phyC and BD-phyC fusion proteins show no interaction with themselves or any other phytochrome in Figure 1B, they are expressed in yeast (Figure 1C). It is possible that these protein fusions do not fold correctly in yeast cells. No evidence for homodimerization of phyE C-terminal sequences is seen in yeast, although phyE interacts with phyD (Figure 1B), demonstrating that phyE C-terminal sequences are capable of binding interactions in this assay. These findings suggest that phyC and phyE may not homodimerize. To further investigate this, full-length phyB, phyC, and phyE proteins were synthesized in vitro and their quaternary structures were assayed by nondenaturing gel electrophoresis. Supplemental Figure 1 online shows that, although phyB migrates as a homodimer in the presence or absence of phycocyanobilin chromophore, neither phyC nor phyE forms a discrete homodimer band.

phyC Forms Only Heterodimers

To test the ability of phyC to bind to itself or to other phytochromes in vivo, transgenes containing epitope-tagged phyC driven by the 35S promoter were introduced into No-0 wild-type *Arabidopsis* (Figure 2A). It has previously been observed that the phyC apoprotein is poorly overexpressed when driven by the 35S promoter but that this additional phyC produces an enlarged leaf phenotype (Qin et al., 1997). Figure 2B shows that phyC tagged with six myc epitopes on either its N (m6-COE) or C terminus (COE-m6) can confer the increased leaf area phenotype. Blot analysis shows that the m6-phyC and phyC-m6 proteins are present at levels similar to endogenous phyC in seedling extracts of these lines, so the transgene products are not substantially overexpressed. Immunoprecipitation (IP) of the extracts with anti-myc antibody pulls down either m6-phyC or phyC-m6 but fails to co-IP native phyC (Figure 2C). The tagged phyC proteins also do not pull down phyA or phyE. However, they both co-IP phyB and very weakly pull down phyD (Figure 2C). These results suggest that phyC does not form homodimers in these lines but, instead, heterodimerizes with phyB and to a small extent with phyD. It should be noted that, throughout this article, extract and IP immunoblot panels in figure panels are not always comparable exposures and cannot be used to directly compare the levels of the phytochromes in one panel with those in other panels. Each panel, however, represents results from a single blot so lanes within panels are directly comparable.

Formation of phyB/phyC heterodimers (phyB/C) and a very weak signal for formation of phyC/D heterodimers was previously observed via IP of epitope-tagged phyB and phyD (Sharrock and Clack, 2004). To confirm that phyC does not bind to itself in vivo,

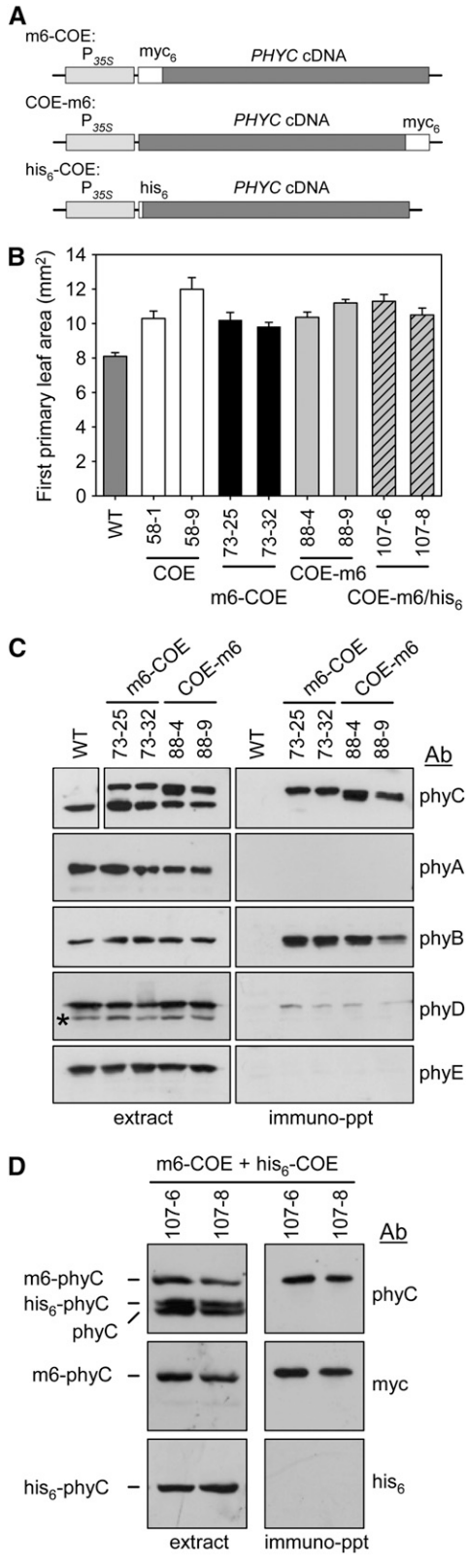

Figure 2. Overexpressed phyC Forms Heterodimers with phyB and phyD but Does Not Homodimerize.

doubly transgenic lines, containing both the m6-COE gene and a 35S:his$_6$-phyC (his$_6$-COE) construct were produced. Figure 2D shows that these lines contain similar levels of the transgene products and native phyC and that IP of m6-phyC from extracts of these plants does not coprecipitate either the native phyC or the his$_6$-phyC.

Expression of m6-phyC from the 35S promoter likely results in that protein being expressed at levels and in cells that are not representative of the normal pattern of the native *PHYC* promoter, and this could affect the IP results. Therefore, transgenes with a *PHYC* upstream promoter region fused to either the β-glucuronidase (GUS) or m6-phyC coding region were introduced into the Columbia (Col) wild-type or Col *phyC-3* mutant backgrounds. The P_{PHYC}-GUS fusion is broadly expressed throughout seedlings, in a pattern similar to the P_{PHYB}-GUS fusion (see Supplemental Figure 2 online). In Figure 3A, the P_{PHYC}:m6-phyC transgene (m6-*PHYC*) is seen to fully complement the red light hypocotyl elongation phenotype of the *phyC-3* null mutant (Monte et al., 2003). Figure 3B shows that IP of m6-phyC from extracts of WT(m6-*PHYC*) lines does not coprecipitate native phyC, confirming that phyC does not bind to itself in planta. However, phyB strongly coprecipitates with m6-phyC irrespective of whether native phyC is present or absent. In addition, as in Figure 2C, phyD very weakly co-IPs with m6-phyC, indicating that phyC can bind to phyD but predominantly dimerizes with phyB. The experiments in Figures 2C and 3B were performed with dark-grown seedlings, while those in Figure 2D were done with light-grown seedlings. Homodimerization of phyC was not detected irrespective of the light conditions.

phyE Forms Only Heterodimers

Yeast two-hybrid experiments indicate that the C terminus of the phyE apoprotein interacts with the phyB and phyD C termini, but not with itself (Figure 1B). To determine the binding characteristics of phyE in vivo, a P_{PHYE}:phyE-myc$_6$ transgene (*PHYE*-m6) was introduced into Landsberg *erecta* (L*er*) wild-type, *phyE*, and *phyB phyE* (abbreviated *phyBE*) host plants. The *phyE* mutation causes early flowering in a *phyB* background (Devlin et al., 1998), but no effect of the *phyE* mutation by itself has been reported. Figure 4A shows that the *phyE* mutant flowers a few days earlier than the wild type under short days and that the *PHYE*-m6 transgene is biologically active; it induces delayed flowering in a

(A) Structures of the three epitope-tagged phyC overexpression (COE) transgenes.

(B) Increased first primary leaf areas of epitope-tagged COE lines. Seedlings were grown for 10 d under continuous white light. Error bars represent the SE of 15 to 20 leaves.

(C) Immunoblot analysis of protein extracts prior to immunoprecipitation (extracts) and of proteins precipitated by the anti-myc antibody (immuno-ppt) from 7-d-old dark-grown seedlings expressing the m6-COE or COE-m6 transgenes. A phyD degradation band present in the extracts is marked with an asterisk.

(D) Immunoblot analysis of 7-d-old light-grown seedling extracts and anti-myc immunoprecipitates from doubly transgenic lines expressing native phyC, myc$_6$-tagged phyC, and his$_6$-tagged phyC.

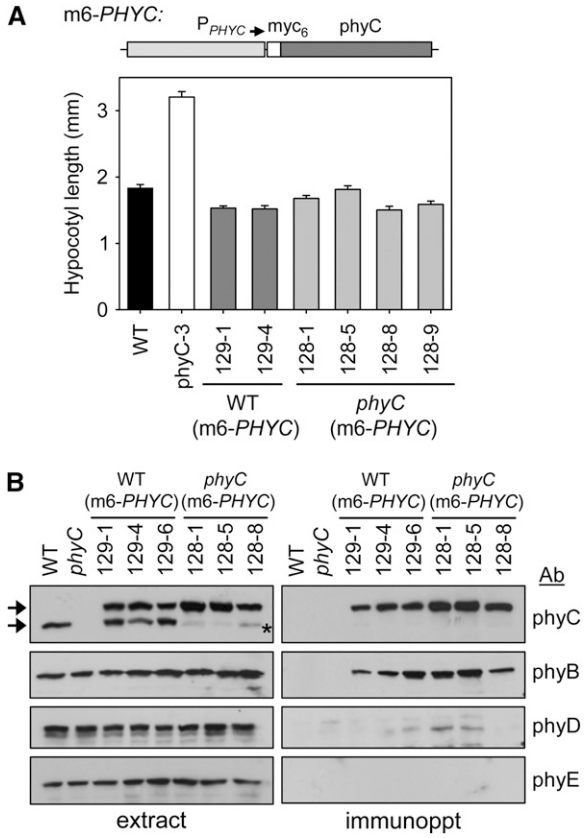

Figure 3. Biological Activity and Heterodimerization of Epitope-Tagged phyC Expressed from Its Native Promoter.

(A) Structure of the m6-*PHYC* transgene and complementation of the *phyC* mutant hypocotyl elongation response under continuous R light. A 3.2-kb region upstream of the start codon of the *PHYC* gene was fused to the myc_6-tagged phyC coding sequence and transformed into the wild-type and *phyC* backgrounds. WT(m6-*PHYC*) and *phyC*(m6-*PHYC*) seedlings were incubated for 3 h white light/21 h dark and then grown for 3 d under R (30 μmol m^{-2} s^{-1}) at 21°C. Error bars represent the SE of 20 to 25 seedlings.

(B) Immunoblot analysis of seedling protein extracts and anti-myc antibody immunoprecipitates from 7-d-old dark-grown wild-type and *phyC* lines expressing the m6-*PHYC* gene. WT(m6-*PHYC*) extracts contain both native phyC and the higher molecular weight myc_6-tagged phyC indicated by arrows. The *phyC*(m6-*PHYC*) extracts contain myc_6-tagged phyC and a degradation band marked with an asterisk.

wild-type background and complements the *phyE* early-flowering phenotype in both the *phyE* and *phyBE* backgrounds. Figure 4B shows that IP of phyE-m6 from extracts of dark-grown WT (*PHYE*-m6) seedlings fails to coprecipitate native phyE but does co-IP phyB and phyD. Co-IP of phyB and/or phyD with phyE-m6 is also observed in the complemented *phyE*(*PHYE*-m6) and *phyBE*(*PHYE*-m6) lines (Figure 4B). Similar results to these were obtained from IP of extracts of light-grown seedlings. Therefore, in seedlings, phyE is present as phyB/E and phyD/E heterodimers but not as a homodimer. Although not quantified, phyD was more readily detected than phyB in the phyE-m6 co-IP fractions in these experiments, suggesting that phyD/E heterodimers likely predominate over phyB/E dimers.

The in Vivo Phytochrome Array

Together with the data presented by Sharrock and Clack (2004), Figures 2 to 4 provide a comprehensive assessment of the in vivo binding of each of the four *Arabidopsis* type II phytochromes to itself, each other, and phyA. Three of the five observed heteromeric complexes of these molecules (phyB/C, phyB/D, and phyB/E) were previously shown by size-exclusion chromatography to migrate at molecular masses characteristic of phytochrome dimers (Sharrock and Clack, 2004), so it is likely that the interaction of phyD with phyC and phyE also results from dimerization of these proteins. No type II phytochrome shows detectable binding interaction with type I phyA. Therefore, we conclude that the phytochrome array in wild-type *Arabidopsis* seedlings consists of homodimers of phyA, phyB, and phyD, the phyB/C, phyB/D, phyB/E, and phyD/E heterodimers, and a very small amount of phyC/D (Figure 4C).

To estimate the relative seedling pool sizes of the different forms of phyB, the amounts of phyB homodimer and phyB-containing heterodimers in extracts of the *phyB*(myc-*PHYB*) line were determined using a quantitative IP approach. In Figure 5, samples from two independent dark-grown seedling anti-myc IPs were separated by electrophoresis along with standard curves of purified apoproteins, and the quantities of each immunoprecipitated phytochrome were determined from immunoblots. In dark-grown *phyB*(myc-*PHYB*) seedlings, the levels of the myc_6-phyB, phyC, phyD, and phyE proteins per 1000 μg of total extract protein were calculated as 60 to 80 ng, 3 to 5 ng, 3 to 4 ng, and 0.5 to 2 ng, respectively (Figure 5). This indicates that, out of the total phyB-containing phytochrome in these dark-grown seedlings, the majority (~85%) is homodimeric, with low levels (2 to 7%) of the three heterodimeric forms. These values are not markedly different from the relative levels of the four type II phytochromes (67% phyB, 13% phyC, 10% phyD, and 10% phyE) previously measured in dark-grown wild-type seedlings (Sharrock and Clack, 2002).

Stability and Quaternary Structure of Excess phyC and phyE

Hirschfeld et al. (1998) observed that the level of phyC phytochrome is decreased fivefold relative to the wild type in *phyB* but not *phyA* mutants. Figure 6A shows that, in diverse *Arabidopsis* L*er* lines containing single or multiple *phy* mutations, reduction in phyC level correlates with presence of a *phyB* null mutation, indicating that, in the absence of its principle binding partner, phyC is destabilized. There is no significant effect of *phyD* or *phyE* mutations by themselves on the level of phyC, but there is a small additive effect of combining the *phyB* and *phyD* mutations (Figure 6A). This suggests that phyD can weakly stabilize phyC by dimerizing with it when phyB is absent. To test whether loss of phyB shifts the dimerization of phyC to other type II phytochromes or even to itself, extracts of *phyB*(m6-COE) lines were immunoprecipitated with the myc antibody. Figure 6B shows that there is no evidence for phyC homodimerization in these lines, but dimerization of the m6-phyC protein with phyD is

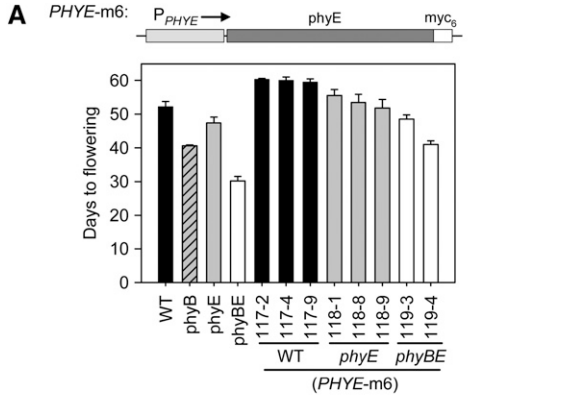

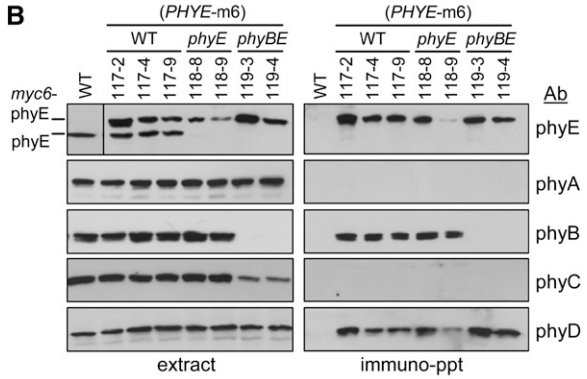

C

Genotype	Phytochrome dimer A/A	B/B	D/D	B/C	B/D	B/E	D/E	C/D
WT	+	+	+	+	+	+	+	±
phyA	—	+	+	+	+	+	+	±
phyB	+	—	+	—	—	—	+	+
phyC	+	+	+	—	+	+	+	—
phyD	+	+	—	+	—	+	—	—
phyE	+	+	+	+	+	—	—	±
phyB phyD	+	—	—	—	—	—	—	—
phyB phyE	+	—	+	—	—	—	—	+
phyB phyD phyE	+	—	—	—	—	—	—	—
phyA phyB	—	—	+	—	—	—	+	+
phyA phyB phyD	—	—	—	—	—	—	—	—
phyA phyB phyD phyE	—	—	—	—	—	—	—	—

Figure 4. Biological Activity and Heterodimerization of Epitope-Tagged phyE.

(A) Structure of the *PHYE*-m6 transgene and complementation of the *phyE* mutant early flowering response. The phyE-myc$_6$ coding sequence was fused to a 1.8-kb *PHYE* promoter region and transformed into the L*er* wild-type, *phyE*, and *phyBE* genetic backgrounds. Plants were grown under short days (8 h light/16 h dark) at 21°C. Error bars represent the SE of 12 plants.
(B) Immunoblot analysis of protein extracts of 7-d-old dark-grown seedlings of the lines from **(A)** prior to immunoprecipitation and of proteins precipitated from those extracts by the anti-myc antibody. Lines expressing the *PHYE*-m6 transgene in the wild-type background contain both native phyE and the higher molecular weight myc$_6$-tagged phyE.
(C) Phytochrome dimer contents of wild-type and *phy* mutant lines. The phytochrome complements that have been demonstrated by in vivo co-IP in the wild-type and *phyB* lines, and those projected for monogenic and selected multiply *phy* mutant lines are summarized. The symbol (±) indicates a very low amount of that dimer form.

increased. Therefore, a *phyB* null mutation in *Arabidopsis* has complex effects. It not only removes homodimeric phyB and a number of phyB/phyX heterodimeric phytochromes but also causes a reduction in the total level of phyC and an increase in the level of the phyC/D heterodimer.

The level of phyE is not altered in single or multiple *phyB* or *phyD* mutants (Figure 6A). Therefore, unlike phyC, absence of its binding partner phytochromes does not destabilize phyE. To test whether the absence of both phyB and phyD causes phyE to

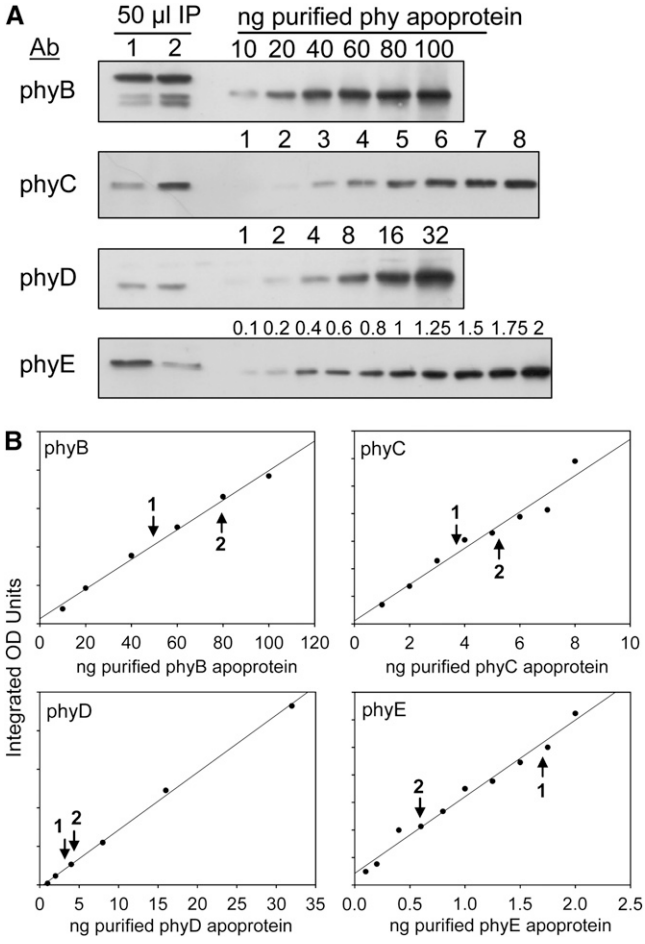

Figure 5. Quantitative Immunoprecipitation Assay for phyB-Containing Dimers.

(A) Immunoblot analysis of anti-myc IP fractions from the *phyB*(myc-*PHYB*) line and standard curves of purified phy apoproteins. Samples of tissue extracts containing 833 µg (sample 1) or 1000 µg (sample 2) of total protein from 7-d-old dark-grown *phyB*(myc-*PHYB*) seedlings were immunoprecipitated with the anti-myc antibody. The immunoprecipitates were separated by SDS-PAGE along with standard curves of purified *Escherichia coli*–expressed phyB–phyE apoproteins. Gels were blotted and probed with the indicated anti-phy antibodies.
(B) Quantification of phytochrome levels in immunoprecipitates. Chemiluminescence signals on autoradiography film images of the immunoblots from **(A)** were scanned and analyzed by densitometry. Arrows labeled 1 and 2 in each panel indicate the values for tissue extract samples 1 and 2 **(A)**.

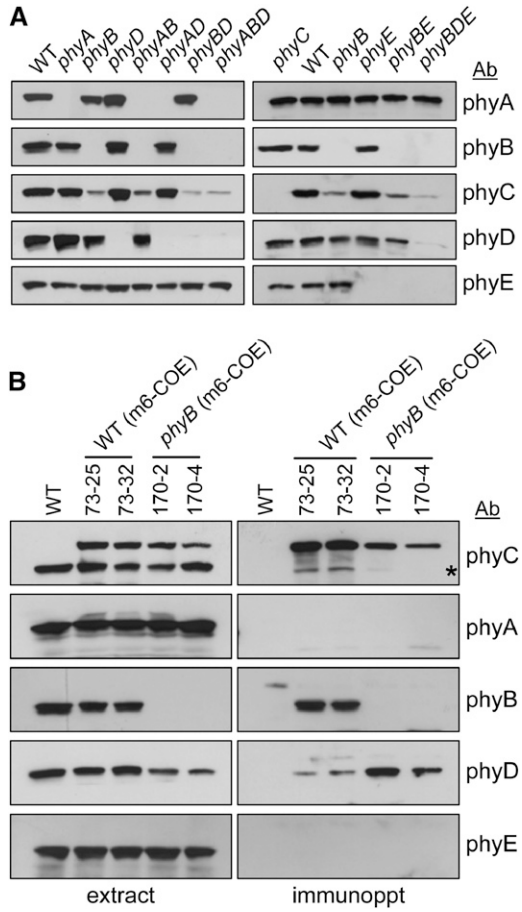

Figure 6. Reduced Overall Levels of phyC but Increased phyC/D Heterodimerization in the *phyB* Mutant.

(A) Immunoblots of the phyA-phyE protein levels in wild-type and *phy* mutant lines. Seedlings were grown for 7 d in the dark, proteins were extracted and separated by SDS-PAGE, and immunoblots were prepared and probed with the indicated anti-phy antibodies.

(B) Immunoblots of extracts and myc antibody IPs of *phyB* mutant lines expressing the m6-COE transgene. Seedlings of the indicated lines were grown for 7 d in the dark, extracts were prepared and immunoprecipitated with anti-myc antibody, and immunoblotting was performed with the anti-phy antibodies. The asterisk indicates a presumed phyC degradation product that does not comigrate with native phyC on gels with higher separation.

either homodimerize or heterodimerize with phyC or phyA, a P_{PHYE}:myc_3-phyE gene was introduced into the L*er phyBD* double mutant. Figure 7A shows that, in these *phyBD*(m3-*PHYE*) lines, the absence of phyB and phyD does not cause m3-phyE to dimerize with native phyE or to heterodimerize with phyC or phyA. This suggests that excess phyE molecules remain monomeric. In Figure 7B, native gel analysis of lines overexpressing each of the five myc_6-tagged phytochromes shows that phyA, phyB, and phyD, which are capable of forming homodimers, are almost exclusively present as dimers. The 35S:m6-phyC line also contains only dimers of the tagged protein, but m6-phyC is not significantly overexpressed (Figures 2C and 2D). By contrast, overexpressed m6-phyE is predominantly present in plant extracts as a monomer, a form that is not present when myc-tagged phyE is expressed at a normal level from the *PHYE* promoter (Figure 7B). Hence, cells treat excess amounts of the two obligately heterodimeric phytochromes, phyC and phyE, in

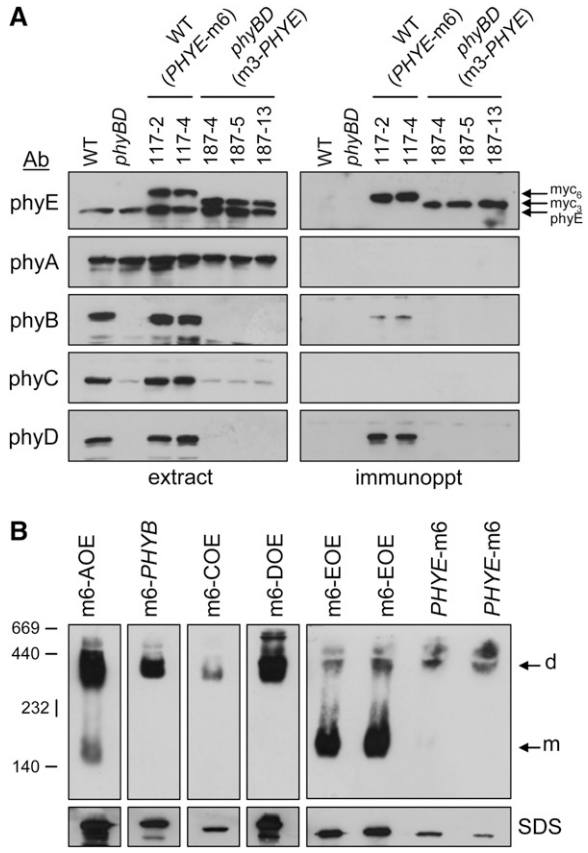

Figure 7. Lack of Dimerization of phyE in the Absence of phyB and phyD and Accumulation of Overexpressed phyE as a Monomer.

(A) Immunoprecipitation of phyE-m6 and myc_3-phyE from seedling extracts of WT(*PHYE*-m6) and *phyBD*(m3-*PHYE*) lines. Seven-day-old dark-grown seedlings of the indicated lines were extracted. Extracts were immunoprecipitated with the myc antibody, and IP samples were fractionated on SDS-PAGE, blotted, and probed with the anti-phy antibodies. Very long exposures of the blots in this experiment did not reveal evidence for dimerization of m3-phyE protein with any potential partner phytochrome in the *phyB phyD* mutant background.

(B) Native gel analysis of nondenatured extracts of seedlings expressing myc-tagged phyA–phyE. 35S promoter–driven overexpression constructs for m6-phyA, m6-phyC, m6-phyD, and m6-phyE were in the No-0 wild-type genetic background. The m6-phyB protein was expressed from the *PHYB* promoter in the No-0 *phyB*(myc-*PHYB*) line, and the phyE-m6 protein was expressed from the *PHYE* promoter in the L*er phyE*(*PHYE*-m6) line. Samples from two independent lines of the epitope-tagged phyE-expressing genotypes were analyzed. Nondenatured extracts were prepared from 7-d-old dark-grown seedlings and fractionated on 4 to 20% native PAGE gels. Blots of the gels were probed with the anti-myc antibody (d, dimer; m, monomer). A small amount of monomeric phyA is seen in the m6-AOE extract. The bottom panel shows a myc antibody-probed immunoblot of an SDS-PAGE gel of the extracts used in the native gel analysis.

different ways: excess phyC is degraded, whereas excess phyE is stable but monomeric.

phyC Is Stabilized but Inactive in the Presence of Chromophoreless phyB Apoprotein

If the instability of phyC in *phyB* mutant lines (Figure 6A) results from lack of its major dimerization partner, expression of chromophoreless phyB containing a Cys357Ser mutation (*PHYB*^{C357S}) in the *phyB* mutant background should restore the phyC level. Figure 8A shows that this in fact occurs. However, expression of chromophoreless phyB does not increase the sensitivity of hypocotyl elongation of the *phyB*(*PHYB*^{C357S}) line relative to the *phyB* mutant over a range of R light fluences (Figure 8B). This indicates that both phyB homodimers consisting of two chromophoreless apoproteins and the presumed phyB^{C357S}/phyC heterodimers that are formed in these lines are inactive. Therefore, phyC requires dimerization with chromophore-bearing phyB to have activity.

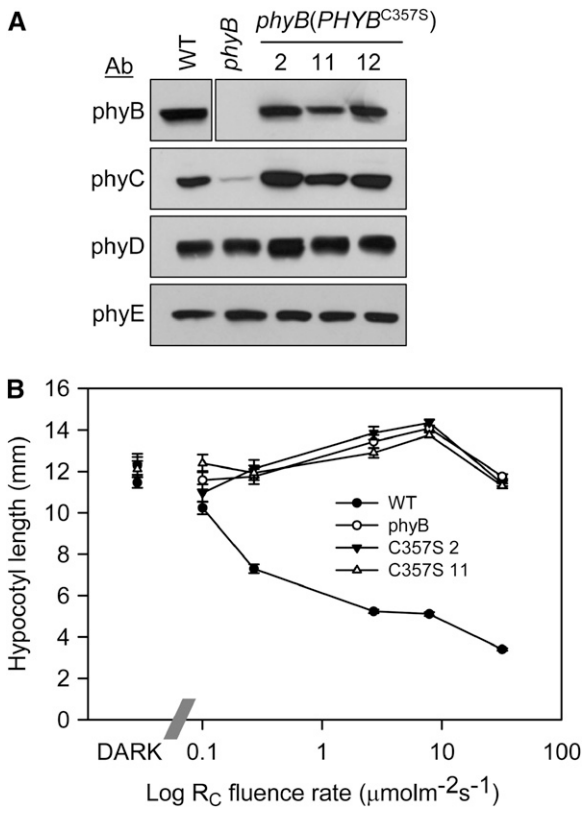

Figure 8. phyC Is Stabilized by the Presence of Chromophoreless phyB but Is Inactive.

(A) Immunoblot analysis of phytochrome levels in *phyB*(*PHYB*^{C357S}) lines. Extracts of 7-d-old dark-grown seedlings were fractionated by SDS-PAGE, blotted, and probed with anti-phy antibodies.

(B) Fluence-response curve for hypocotyl length in 6-d-old *phyB* (*PHYB*^{C357S}) lines grown under continuous R. Mean and SE values are representative of at least 20 seedlings for each light treatment.

Activities of phyC and phyE in the Absence of Their Dimerization Partners

As illustrated in Figure 4C, one prediction of the dimerization profiles of phyC and phyE is that the light response deficiencies of *Arabidopsis phyC* and *phyE* null mutants result from a lack of specific phytochrome heterodimers. Moreover, unless phyC or phyE monomers have biological activity, mutational loss of their binding partner phys should disrupt the activities of either of these two photoreceptors. It is predicted that a *phyBD* double mutant completely lacks type II phytochrome homo- and heterodimers (Figure 4C) and should be phenotypically identical to *phyBCD*, *phyBDE*, and *phyBCDE* multiple mutants. Although not all combinations of *phy* mutations have been constructed, it appears that this prediction is not borne out. Figure 9 shows flowering times under short days and hypocotyl lengths under R of *phyB*, *phyD*, and *phyE* mutants and lines containing combinations of these mutations. The *phyB* and *phyE* mutants flower early relative to the wild type, and combination of *phyB* with either *phyD* or *phyE* exacerbates this phenotype. This is consistent with loss of the predicted phytochrome forms in these lines (Figure 4C). However, the *phyBDE* triple mutant flowers several days earlier than the *phyBD* double mutant, illustrating that, in the absence of its phyB and phyD dimerization partners, phyE has biological activity. Relative to the *phyBD* line, the *phyBDE* triple mutant also has elongated hypocotyls under R at the seedling stage (Figure 9). It has previously been observed that these two lines differ in flowering time at 16°C and that the *phyABDE* quadruple mutant flowers early and has altered expression of the *FLOWERING LOCUS T* mRNA relative to the *phyABD* triple mutant at 16°C (Halliday et al., 2003). These light responses demonstrate that a small flux of signaling activity through pathways involving phyE, mediated either by undetected amounts of homodimers of this protein or by activity of phyE monomers, can have physiological effects.

Similar reasoning suggests that, because phyC forms only heterodimers, a *phyABDE* quadruple mutant should contain no dimeric phytochrome (Figure 4C). However, *phyABDE* does not develop under continuous R with a completely etiolated phenotype; it has very small but significant increases in cotyledon area and angle under R compared with in the dark (Franklin et al., 2003b). Hence, a small sensitivity to R remains in *Arabidopsis* seedlings that contain only phyC. Again, whether this is mediated through undetected phyC homodimers or phyC monomers is not known.

Phytochrome Heterodimers Interact with the PIF3 bHLH Protein in Vivo in an R/FR-Dependent Manner

A line expressing a 35S:PIF3-myc$_6$ transgene (PIF3-m6) was constructed and, as previously observed (Kim et al., 2003), showed hyposensitivity to R light (see Supplemental Figure 3 online). Extracts of seedlings of this line harvested over a 10-min time course following a 30-s pulse of R were prepared and immunoprecipitated with the anti-myc antibody. Figure 10A shows that, by 10 min following the R pulse, the PIF3-m6 protein is shifted in migration, due to phosphorylation (Al-Sady et al., 2006), and is beginning to be degraded as previously observed

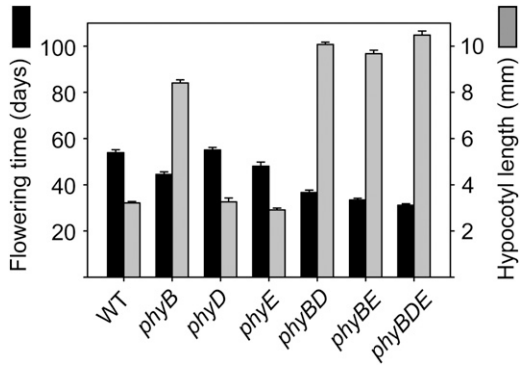

Figure 9. Light Responses of Mutants Lacking Selected Combinations of Phytochrome Dimers.

Flowering times under an 8-h-light/16-h-dark photoperiod and hypocotyl lengths of 5-d-old seedlings grown under continuous R (30 μmol m^{-2} s^{-1}) were measured for the indicated lines. Error bars represent the SE for 12 plants and 20 to 25 seedlings, respectively.

for native PIF3 (Bauer et al., 2004; Park et al., 2004; Al-Sady et al., 2006). By 1 min after the R pulse, phyA, phyB, phyC, and phyD are all detected in the PIF3-m6 immunoprecipitate, whereas they are not detected in control samples from untransformed lines or from the non-R-treated samples (Figure 10A). Therefore, all of the phytochromes, with the possible exception of phyE, bind either directly or indirectly to PIF3 upon their conversion to Pfr in vivo.

phyA and phyB synthesized in vitro and assembled with a phycocyanobilin chromophore co-IP selectively in their Pfr forms with a GAL4-PIF3 fusion protein, indicating that these two phys bind directly to PIF3 after exposure to light (Zhu et al., 2000). In addition, the isolated PIF3 APB domain binds in vitro to phyB but not to phyC or phyD (Khanna et al., 2004). Therefore, the association of the Pfr forms of phyC and phyD with PIF3 in vivo (Figure 10A) more likely results from PIF3 binding to phyB/C and phyB/D heterodimers through their phyB subunits than from direct phyC-to-PIF3 and phyD-to-PIF3 binding. The immunoprecipitate panels for the anti-phy antibodies in Figure 10 are from long exposures of chemiluminescent blots to film, suggesting that only a small fraction of each of these phytochromes is interacting with PIF3. This is expected because PIF3 is predominantly nuclear (Ni et al., 1998), and, in dark-grown seedlings treated with a R pulse, only a small fraction of each of the phytochromes is located in the nucleus (Kircher et al., 2002). Colocalization of phyB–yellow fluorescent protein (YFP) with PIF3–cyan fluorescent protein in nuclear bodies occurs within 2 min of exposure to R (Bauer et al., 2004), indicating that interaction of these proteins within the nucleus can be rapidly induced by light. However, it cannot be ruled out that, if a small fraction of PIF3 is in fact localized to the cytoplasm, the phyA–phyD that co-IP with PIF3-m6 in Figure 10A could be from the cytosolic phytochrome pools. Either way, it is expected that the majority of PIF3 molecules and the majority of each of the phytochromes are not in the same cellular compartment under the conditions of this experiment, so their interaction should be limited. Of all of the phytochromes, phyC is the most readily detected as binding to PIF3, perhaps because of high specificity and titer of the anti-phyC antibody. Immunoprecipitation data obtained up to this time for phyE interaction with PIF3-m6 in vivo are inconclusive (Figure 10A).

Figure 10B shows that, using 15-s pulses of light, induction by R of co-IP of phyA, phyB, phyC, and phyD with PIF3-m6 is at least partially reversible with FR. Since phyC is present in

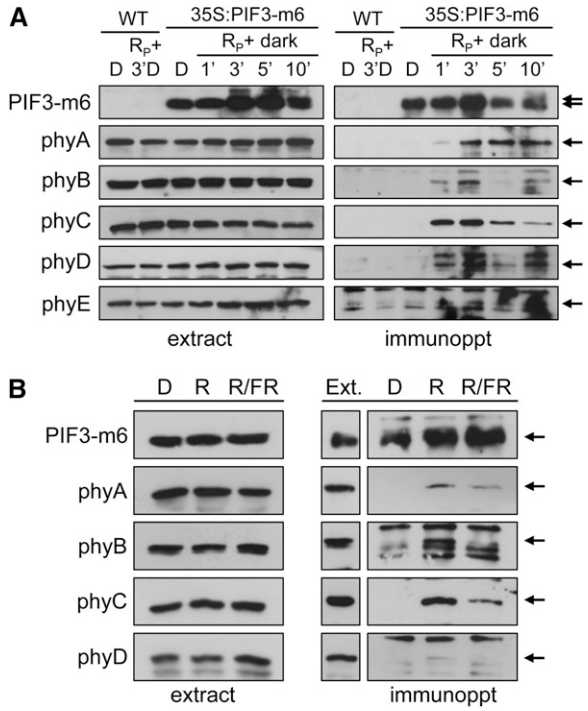

Figure 10. R/FR-Reversible Co-IP of Phytochromes with PIF3-myc_6 from Seedling Extracts.

(A) Rapid binding of phyA, phyB, phyC, and phyD to PIF3-m6 following a pulse of R light.

Five-day-old dark-grown wild-type and 35S:PIF3-myc_6 seedlings were kept in the dark (D) or exposed to a 30-s pulse of R (30 μmol m^{-2} s^{-1}) and returned to the dark. The R-pulsed 35S:PIF3-m6 seedlings were harvested over the indicated 10-min time course, and one R-pulsed wild-type sample was harvested at 3 min following return to the dark. Protein extracts were prepared and IP performed with the anti-myc antibody. Samples of the immunoprecipitates were fractionated by SDS-PAGE, blotted, and probed with the anti-myc antibody to detect PIF3-m6 or with the anti-phy antibodies. Arrows to the right of the blot panels indicate the positions of the respective antigens. The two arrows to the right of the PIF3-m6 panels indicate the positions of presumed phosphorylated (top arrow) and unphosphorylated (bottom arrow) PIF3-m6 (Al-Sady et al., 2006).

(B) FR reversibility of R-induced phy-PIF3 binding. Five-day-old dark-grown 35S:PIF3-myc_6 seedlings were kept in the dark, exposed to 15 s of R (30 μmol m^{-2} s^{-1}) or 15 s R followed by 15 s FR (39 μmol m^{-2} s^{-1}), returned to the dark, and harvested 3 min later. Proteins were extracted and immunoprecipitated with anti-myc antibody. IP samples were fractionated by SDS-PAGE, and immunoblots were probed with the anti-myc or anti-phy antibodies. The IP blots on the right include parallel blots of the dark extract (Ext.) that were fractionated on the same PAGE gels as the IP samples to provide size standards for the phy proteins.

seedling extracts as a heterodimer, these results demonstrate that phytochrome heterodimers interact with PIF3 in an R/FR-reversible manner and likely function through PIF-mediated pathways.

DISCUSSION

Since the initial description of multiple forms of phytochrome in plants (Sharrock and Quail, 1989), there has been a prevailing assumption that, as was originally shown for purified native phyA (Jones and Quail, 1986), all phytochromes in cells exist as homodimers. This assumption was challenged by the identification of phy heterodimers in *Arabidopsis* seedling extracts (Sharrock and Clack, 2004). Here, by testing the binding specificities of all of the *Arabidopsis* phytochromes using yeast two-hybrid and co-IP analyses, we conclude that in fact heterodimerization of plant phys is common. More remarkably, there is no evidence for homodimerization of phyC or phyE, indicating that these two forms are present in cells only as heterodimers with phyB or phyD. These observations lead to a revision of the model for the higher-plant R/FR-sensing photoreceptor array and have important implications for the interpretation of phenotypes of the *phy* mutants and phy overexpresser lines that have been central to defining plant photoreceptor functions and interactions. Figure 4C shows a summary of the phytochrome contents of wild-type *Arabidopsis* and a number of *phy* mutants and mutant combinations. With regard to other species, it will be interesting to determine whether phyB and phyC, which are present in most dicots and monocots, always form a heterodimer and whether any gymnosperm phys also show this property.

It is likely, though not yet directly shown, that all of the higher-plant phys attach the same phytochromobilin chromophore and that differences in the photosensing and regulatory activities of the phyA-E receptor types reflect differences in their respective apoprotein sequences. The *PHY* gene family has changed and expanded over the course of angiosperm evolution (Mathews, 2006). The progenitor *PHYA*, *PHYB*, and *PHYC* genes diverged early, as most angiosperms contain these three homologs, and their products are similarly divergent in amino acid sequence (~50% identity). The *PHYE* gene arose later, by duplication of *PHYB*, but probably early in the dicot lineage. Our findings suggest that *PHYC* and *PHYE* evolved to encode proteins that function in physical association with *PHYB* and *PHYB*-like gene products, increasing the diversity of R/FR receptor types in a combinatorial way. The *PHYD* gene arose via a much later duplication of *PHYB* in *Brassicaceae* (Mathews and McBreen, 2008). Like phyB, phyD can heterodimerize with phyC and phyE. From these considerations, we propose that phyB and phyD constitute the core type II phytochrome subunits through which type II phy function is mediated. Moreover, since formation of the phyB^{C357S}/phyC heterodimer does not significantly alter the sensitivity of the *phyB* mutant to R, it is likely that phyC subunits require active phyB core partners to be active themselves.

Yeast two-hybrid analyses indicate that the *Arabidopsis* phytochrome homomeric and heteromeric subunit interactions are mediated by sequences in the C-terminal halves of the apoproteins. This is consistent with previous observations that deletion of the C-terminal 200 amino acids of oat (*Avena sativa*) phyA or the C-terminal 470 amino acids of *Arabidopsis* phyB generates monomeric photoactive N-terminal phy fragments in vivo (Cherry et al., 1993; Wagner et al., 1996). Cyanobacterial, eubacterial, and fungal phytochromes have C-terminal domains that function as light-regulated two-component histidine kinases, whereas plant phys have unique C termini that contain two PAS domains and a region homologous to two-component histidine kinases but lacking residues critical to HK activity (Sharrock, 2008). The phyB C terminus is required for light-induced nuclear localization and nuclear body formation (Chen et al., 2005). Our findings demonstrate that this region of plant phys is also critical for intrasubunit contacts that determine dimer structure and heterogeneity. Moreover, in *phyB*(*PHYB*^{C357S}) lines, phyC subunits are stabilized by and presumably bound to chromophoreless phyB subunits but lack light-sensing activity. This suggests that dimerization and intrasubunit interactions are integral to phy signaling mechanisms.

The light-dependent phenotype of *phyB* null mutants is much stronger than that of monogenic *phyC*, *phyD*, or *phyE* null mutants. The *phyB* phenotype includes deficiencies in R/FR-regulated hypocotyl elongation, hook opening, cotyledon and leaf expansion, flowering time, gene expression, and circadian timing (Somers et al., 1991; Reed et al., 1993). The monogenic *phyC*, *phyD*, and *phyE* mutants show similar but milder alterations in subsets of those light responses (Aukerman et al., 1997; Devlin et al., 1998; Franklin et al., 2003a; Monte et al., 2003). We have shown that the majority of phyB is present in seedlings as phyB/B homodimers, but 2 to 7% is present as each of the phyB/C, phyB/D, and phyB/E heterodimers. Considering the levels of the various phy proteins present in seedlings (Sharrock and Clack, 2002), these proportions are consistent with approximately equivalent probabilities of a phyB subunit dimerizing with any of its four partners. Although phyB/B homodimers appear to have stronger overall activity than any of the individual heterodimers, it may be difficult to predict the selective value of individual photoreceptor function. For example, when analyzed under laboratory conditions, *phyB* mutants flower early under most photoperiods, but *phyC* mutants do not, suggesting that phyB/C heterodimers play only a minor role in this response (Franklin et al., 2003a; Monte et al., 2003). However, polymorphism at the *PHYC* gene accounts for significant variation in flowering time, and growth responses among *Arabidopsis* ecotypes and different naturally occurring *PHYC* alleles, presumably functioning through phyB/C heterodimers, are subject to diversifying selection (Balasubramanian et al., 2006).

The instability of phyC in *phyB* null-containing mutants, accompanied by a concurrent increase in the low-abundance phyC/D heterodimer, and formation of phyE monomers when that protein is overexpressed lend support to a model for phytochrome structural diversity that has obligate heterodimerization as a major component. Nevertheless, there are some inconsistencies between the proposed phy contents of some of the *Arabidopsis* mutant lines in Figure 4C and the light response phenotypes of those lines. For example, pairs of multiple mutants that should completely lack type II phy dimers but differ in the presence or absence of a *phyE* mutation (*phyBD* versus *phyBDE* and *phyABD* versus *phyABDE*) show small differences in light

response (Figure 9; Franklin et al., 2003b; Halliday et al., 2003; Halliday and Whitelam, 2003). In addition, the *Arabidopsis phyABDE* quadruple mutant retains a slight sensitivity to R for cotyledon expansion and induction of *ATHB-2* gene transcription (Franklin et al., 2003b). These observations indicate that phyC and phyE have some signaling activity in the absence of their known dimerization partners. It is not known whether this weak partner-independent function results from the activity of phyC and phyE monomers or from pools of phyC and phyE homodimers that we have been unable to detect.

There is a great deal of evidence for direct light-regulated interaction of phyA and phyB with downstream signaling proteins (Castillon et al., 2007; Quail, 2007; Bae and Choi, 2008). One major group of these proteins consists of the members of the PIF/PIL bHLH family. The archetypal phytochrome binding bHLH protein, PIF3, was shown to bind differentially in vitro to phyA and phyB in their Pfr conformations (Ni et al., 1999; Zhu et al., 2000). PIF3 is rapidly phosphorylated and degraded in vivo after a pulse of R, and the *pif3* mutant is hypersensitive to R at the seedling stage (Bauer et al., 2004; Monte et al., 2004; Park et al., 2004). These findings demonstrate that PIF3 primarily functions during deetiolation as a negative regulator of photomorphogenesis, although a positive role for PIF3 in rapidly phy-induced regulation of gene expression has also been shown (Al-Sady et al., 2008). The PIF1/PIL5, PIF3, PIF4, PIF5/PIL6, PIF6/PIL2, and PIF7 bHLH proteins all function downstream of phyA and/or phyB, and mutations in the genes encoding these proteins result in defective light-sensing phenotypes. Like PIF3, the PIF1, PIF4, and PIF5 proteins are phosphorylated and degraded in R (Shen et al., 2007; Lorrain et al., 2008; Shen et al., 2008). In addition, PIF3 and PIF7 colocalize with phyA or phyB in nuclear bodies (Bauer et al., 2004; Al-Sady et al., 2006; Leivar et al., 2008). However, only one bHLH protein has previously been shown by co-IP to interact with phytochrome in a light-regulated manner in vivo; PIF1 R/FR-reversibly co-IPs phyA and phyB (Shen et al., 2008). We have demonstrated, using co-IP from seedling extracts, that PIF3 binds, either directly or indirectly, to phyA, B, C, and D within the first few minutes after a 15- or 30-s pulse of R and that this binding is partially reversed if the R pulse is followed by a FR pulse. These results provide direct evidence for light-regulated phy-PIF3 interaction in vivo. They also show that PIF3 binds to both homodimeric and heterodimeric phytochromes because phyA is present only as a homodimer and phyC is present only as a heterodimer in the seedling extracts. Khanna et al. (2004) demonstrated that the PIF3 APB domain binds in vitro to phyB but not phyC or phyD. Therefore, it is likely that the phyC and phyD molecules that coprecipitate with PIF3 in Figure 10 are pulled down as a result of PIF3 binding to phyB subunits present in phyB/C and phyB/D heterodimers. Nevertheless, these results suggest that all phytochromes, with the possible exception of phyE-containing forms, signal at early stages of deetiolation through PIF proteins.

Experiments monitoring the localization of phy–green fluorescent protein fusions indicate that the majority of each of the five *Arabidopsis* phys is present in the cytoplasm of dark-grown seedlings and that a brief pulse of R is not sufficient to cause detectable movement of these cytoplasmic proteins to the nucleus (Kircher et al., 2002; Kevei et al., 2007). However, in the same experiments, the phy–green fluorescent protein fusions of type II phyB-E all show some fluorescence in nuclei of etiolated cells, suggesting that a small fraction of these phys is constitutively nuclear. Following transfer from dark to continuous R, phyB-YFP and phyD-YFP colocalize with PIF3–cyan fluorescent protein within minutes (Bauer et al., 2004). The time courses of in vivo PIF3-m6 interaction with phyA, B, C, and D presented here are consistent with those observations, showing that these four phys can be pulled down by PIF3-m6 within a minute after an R pulse and that these interactions peak at ~3 min after the light pulse. This supports a model in which the Pfr forms of small fractions of the diverse phy dimer forms, either rapidly translocated from the cytoplasm to the nucleus upon exposure to light or present in the nucleus prior to light-induced nuclear import of larger amounts of the phys, bind to members of the PIF bHLH family and mediate rapid R/FR responses. These findings contribute to a growing understanding of photoreceptor function and early transduction events in light signaling pathways.

METHODS

Plant Growth, Measurement, and Histochemical Staining

The *Arabidopsis thaliana phyB-1*, *phyD-1*, and *phyE-1*mutant lines and the multiply mutant lines generated from these are in the L*er* genetic background (Aukerman et al., 1997; Devlin et al., 1998; Franklin et al., 2003b). The *phyC-3* mutant is in the Col background (Monte et al., 2003). Seeds were surface sterilized and planted on Murashige and Skoog medium containing 0.8% agar without sucrose. The plates were incubated in the dark for 3 d at 4°C, exposed to fluorescent light at room temperature for 3 h to induce uniform germination, and then transferred to the growth conditions described in the figure legends. R (670 nm) and FR (735 nm) light were supplied by LEDs in an E-30LED growth chamber (Percival). Hypocotyl lengths were determined by laying out at least 20 seedlings per treatment on 0.8% agar plates, photographing them, and measuring the hypocotyls using ImageJ software (National Institutes of Health). First primary leaf areas were measured by excising these organs from 10-d-old seedlings grown under fluorescent light (60 μmol m^{-2} s^{-1}), placing them on agar plates, and determining their areas using ImageJ. Flowering experiments were conducted in a growth chamber (Conviron) containing fluorescent bulbs (160 μmol m^{-2} s^{-1}) at 21°C. Flowering time was measured as the day on which the first floral bud became visible at the center of the rosette. Histochemical staining of seedlings for GUS activity was performed as described (Goosey et al., 1997).

Plasmid Construction and Plant Transformation

All plant transformation plasmids were constructed in vectors derived from pBI123 (Sharrock et al., 2003a). These carried selectable marker genes encoding kanamycin resistance, designated pBI clones, or gentamicin resistance, designated pGNT clones. Full-length *PHYA*, *PHYB*, *PHYC*, and *PHYD* cDNA sequences from the Col ecotype and a *PHYE* cDNA sequence from the L*er* ecotype were used in construction of all recombinant clones. The *phyB*(myc-*PHYB*) and WT(myc-DOE) lines were as described (Sharrock and Clack, 2004). The *PHYB*, *PHYC*, and *PHYE* cDNA sequences were translationally fused at their N termini or their C termini to the myc_6, his_6, or myc_3 epitope tags and placed under the control of the 35S promoter, a *PHYC* gene promoter region, or the *PHYB* or *PHYE* gene promoters previously described (Goosey et al., 1997), as indicated for each construct. DNA sequences, relevant restriction sites,

and protein reading frames of the N-terminal and C-terminal cloning junctions from the epitope-tagged transgenes are presented in Supplemental Figure 4 online. DNA oligonucleotides used in construction of recombinant genes are listed in Supplemental Table 1 online. The *PHYC* promoter fragment contained 3149 bp of Col genomic sequence upstream of the ATG start codon. For the P_{PHYC}:GUS transgene, a fragment containing the 3.15-kb *PHYC* promoter and the first 21 amino acids of the phyC polypeptide was translationally fused to the GUS sequence. The $PHYB^{C357S}$ transgene was identical to the P_B-phyB construct (Sharrock et al., 2003b) except for a G-to-C substitution at base pair 1070 of the phyB coding sequence, changing the chromophore attachment site Cys-357 to a Ser. Site-directed mutagenesis was performed with a QuikChange Lightning kit (Stratagene). The PIF3 coding sequence was amplified by RT-PCR from Col wild-type dark-grown seedling cDNA, prepared with a SuperScript III cDNA kit (Invitrogen).

Plant transformations were performed by the floral dip method using *Agrobacterium tumefaciens* strain GV3101. The pBI-35S:myc_6-phyC (m6-COE), pBI-35S:phyC-myc_6 (COE-m6), and pGNT-35S:his_6-phyC (his_6-COE) T-DNA regions were transformed into No-0 wild type, and the pBI-35S:myc_6-phyC (m6-COE) construct was also transformed into No-0 *phyB-1*. The pBI-P_{PHYC}:myc_6-phyC (m6-*PHYC*) construct was transformed into Col wild type and *phyC-3*. The pBI-P_{PHYE}:phyE-myc_6 (*PHYE*-m_6) T-DNA region was transformed into the L*er* wild-type, *phyE-1*, *phyB-1 phyD-1*, and *phyB-1 phyE-1* backgrounds. The pBI-P_{PHYE}:myc3-phyE (m3-*PHYE*) gene was transformed into L*er phyB-1 phyD*-1. The *PHYE* promoter fragment consisted of 1.8 kb of genomic sequence upstream of the phyE start codon. The pBI-P_{PHYB}:$phyB^{Cys357Ser}$ ($PHYB^{C357S}$) T-DNA was transformed into No-0 *phyB-1*, and the pBI-35S:myc_6-phyA (m6-AOE) and pBI-35S:myc_6-phyE (m6-EOE) constructs were transformed into No-0 wild type. pBI-35S:PIF3-myc6 was transformed into the Col wild type. In each of these transformations, multiple independent homozygous T3 lines expressing the *PHY* transgene were identified and used in experiments.

Protein Extraction, Immunoprecipitation, Immunoblots, and Native Gel Electrophoresis

Seedling protein extracts were prepared, and IPs were performed with the anti-myc 9E10 antibody as described (Sharrock and Clack, 2004). Seedling extract and IP samples were analyzed by 6% SDS-PAGE, immunoblotting, and detection of antigen with the monoclonal antibodies anti-myc 9E10, anti-phyA 073d, anti-phyB B6B3, anti-phyC C11 and C13, anti-phyD 2C1, and anti-phyE 7B3 (Hirschfeld et al., 1998). The his_6 tag was detected with the RGS-His antibody (Qiagen). Dilutions of the primary antibodies were from 1:200 to 1:2000 and were determined empirically for each antibody sample. Chemiluminescent detection of primary antibodies was performed with horseradish peroxidase–conjugated secondary antibody and Supersignal West Pico reagents (Thermo Fisher Scientific). For each IP experiment, a set of gel lanes was loaded with the protein extract on the basis of protein concentration and a set of gel lanes was loaded with IP samples as equivalent volumes from precipitations performed in parallel. For native gel electrophoresis, 7-d-old dark-grown seedlings were ground at 0°C under dim green safe light at a 1:1 weight: volume ratio in nondenaturing extraction buffer (25 mM Tris-HCl, pH 7.5, 10 mM NaCl, and 5 mM EDTA) containing Complete EDTA-free Protease Inhibitor Cocktail (Roche Diagnostics), and the extracts were centrifuged for 3 min at 4°C. Proteins were separated on 4 to 20% gradient PAGE gels in Tris/borate/EDTA buffer for 40 h at 4°C. Gel blotting and probing with the myc antibody were the same as for SDS-PAGE gels. Yeast protein extracts were prepared using the urea/SDS method in the Yeast Protocols Handbook of the Matchmaker GAL4 System 3 (Clontech). Anti-GAD antibody (Clontech) was used at 1:1000 dilution and was detected by chemiluminescence as described above.

Quantitative Immunoprecipitation Assay

Seedlings of the *phyB*(myc-*PHYB*) line (Sharrock and Clack, 2004) were grown for 7 d in darkness, extracted, and immunoprecipitated as two independent replicate experiments. Samples of tissue extracts containing 833 μg of total protein from the first experiment and 1000 μg from the second experiment were immunoprecipitated with the anti-myc antibody and fractionated by 6% SDS-PAGE along with standard curves of purified *Escherichia coli*–expressed phyB–phyE apoproteins (Sharrock and Clack, 2002). Gels were blotted to nitrocellulose and probed with the anti-phy antibodies. Immunoblot chemiluminescence signals on autoradiography film were scanned and quantified by densitometry (Sharrock and Clack, 2002).

Yeast Two-Hybrid Assay

Yeast two-hybrid assays were performed with materials and protocols from the Matchmaker GAL4 System 3 (Clontech). Regions from the *PHY* cDNA sequences encoding the following phy amino acid sequences were PCR amplified and cloned into the pGAD-T7 and pGBK-T7 vectors: phyA C-550 (D589-K1122) and phyA C-200 (Q930-K1122), phyB C-550 (E620-Y1172) and phyB C-200 (Q962-Y1172), phyC C-550 (Q578-I1111) and phyC C-200 (Q917-I1111), phyD C-550 (E624-S1164) and phyD C-200 (S955-S1164), and phyE C-550 (R570-K1112) and phyE C-200 (Q905-K1112). Primers used in PCR are listed in Supplemental Table 1 online. Assays were performed under room light conditions.

In Vitro Transcription and Translation

By introducing *Nde*I sites at their ATG start codons (see Supplemental Table 1 online), the full-length *Arabidopsis* Col wild-type *PHYB* and *PHYC* cDNA sequences were cloned into the pET3c expression vector and the L*er* wild-type *PHYE* cDNA sequence was cloned into the pET-30a expression vector (Novagen). Plasmid DNA samples were amplified with primers 5′-TCCCGCGAAATTAATACGAC-3′ and 5′-CCGGATA-TAGTTCCTCCTTTCA-3′ to produce template PCR fragments, and these were transcribed and translated in the presence of ^{35}S-methionine using reagents and protocols from the TNT T7 Quick for PCR DNA kit (Promega). Following incubation for 90 min at 30°C for transcription/translation, 10 μM 3E-phycocyanobilin was added to some reactions, and incubations at 30°C were performed for an additional 90, 180, and 270 min. Labeled reactions were fractionated on 4 to 20% nondenaturing PAGE gels, dried, and exposed to autoradiography film. Phycocyanobilin was prepared from lyophilized *Spirulina patensis* (Terry et al., 1993).

Accession Numbers

Sequence data from this article can be found in the Arabidopsis Genome Initiative or GenBank/EMBL databases under the following accession numbers: PHYA (AT1G09570), PHYB (AT2G18790), PHYC (AT5G35840), PHYD (AT4G16250), PHYE (AT4G18130), and PIF3 (AT1G09530).

Supplemental Data

The following materials are available in the online version of this article.

Supplemental Figure 1. Native Gel Analysis of in Vitro–Translated phyB, phyC, and phyE with and without Phycocyanobilin Chromophore.

Supplemental Figure 2. Histochemical Localization of P_{PHYB}:GUS and P_{PHYC}:GUS Expression in Light-Grown Seedlings.

Supplemental Figure 3. Hypocotyl Lengths of Wild-Type and the 35S:PIF3-myc6 Transgenic Line Grown for 7 d under 25 μmol m^{-2} s^{-1} Continuous Red Light.

Supplemental Figure 4. Sequences of *PHYC*, *PHYE*, *PHYA*, and *PIF3* Epitope-Tagged Transgene Cloning Junctions.

Supplemental Table 1. Oligonucleotide Primers.

ACKNOWLEDGMENTS

We thank Peter Quail and Garry Whitelam for providing genetic stocks. This work was supported by grant IBN-0348913 to R.A.S. from the National Science Foundation.

Received December 17, 2008; revised February 17, 2009; accepted March 2, 2009; published March 13, 2009.

REFERENCES

Al-Sady, B., Kikis, E.A., Monte, E., and Quail, P.H. (2008). Mechanistic duality of transcription factor function in phytochrome signaling. Proc. Natl. Acad. Sci. USA **105:** 2232–2237.

Al-Sady, B., Ni, W., Kircher, S., Schafer, E., and Quail, P.H. (2006). Photoactivated phytochrome induces rapid PIF3 phosphorylation prior to proteasome-mediated degradation. Mol. Cell **23:** 439–446.

Aukerman, M.J., Hirschfeld, M., Wester, L., Weaver, M., Clack, T., Amasino, R.M., and Sharrock, R.A. (1997). A deletion in the *PHYD* gene of the Arabidopsis Wassilewskija ecotype defines a role for phytochrome D in red/far-red light sensing. Plant Cell **9:** 1317–1326.

Bae, G., and Choi, G. (2008). Decoding of light signals by plant phytochromes and their interacting proteins. Annu. Rev. Plant Biol. **59:** 281–311.

Balasubramanian, S., Sureshkumar, S., Agrawal, M., Michael, T.P., Wessinger, C., Maloof, J.N., Clark, R., Warthmann, N., Chory, J., and Weigel, D. (2006). The PHYTOCHROME C photoreceptor gene mediates natural variation in flowering and growth responses of *Arabidopsis thaliana*. Nat. Genet. **38:** 711–715.

Bauer, D., Viczian, A., Kircher, S., Nobis, T., Nitschke, R., Kunkel, T., Panigrahi, K.C., Adam, E., Fejes, E., Schafer, E., and Nagy, F. (2004). Constitutive photomorphogenesis 1 and multiple photoreceptors control degradation of phytochrome interacting factor 3, a transcription factor required for light signaling in Arabidopsis. Plant Cell **16:** 1433–1445.

Castillon, A., Shen, H., and Huq, E. (2007). Phytochrome interacting factors: Central players in phytochrome-mediated light signaling networks. Trends Plant Sci. **12:** 514–521.

Chen, M., Tao, Y., Lim, J., Shaw, A., and Chory, J. (2005). Regulation of phytochrome B nuclear localization through light-dependent unmasking of nuclear-localization signals. Curr. Biol. **15:** 637–642.

Cherry, J.R., Hondred, D., Walker, J.M., Keller, J.M., Hershey, H.P., and Vierstra, R.D. (1993). Carboxy-terminal deletion analysis of oat phytochrome A reveals the presence of separate domains required for structure and biological activity. Plant Cell **5:** 565–575.

Devlin, P.F., Patel, S.R., and Whitelam, G.C. (1998). Phytochrome E influences internode elongation and flowering time in Arabidopsis. Plant Cell **10:** 1479–1487.

Edgerton, M.D., and Jones, A.M. (1992). Localization of protein-protein interactions between subunits of phytochrome. Plant Cell **4:** 161–171.

Essen, L.O., Mailliet, J., and Hughes, J. (2008). The structure of a complete phytochrome sensory module in the Pr ground state. Proc. Natl. Acad. Sci. USA **105:** 14709–14714.

Franklin, K.A., Davis, S.J., Stoddart, W.M., Vierstra, R.D., and Whitelam, G.C. (2003a). Mutant analyses define multiple roles for phytochrome C in Arabidopsis photomorphogenesis. Plant Cell **15:** 1981–1989.

Franklin, K.A., Praekelt, U., Stoddart, W.M., Billingham, O.E., Halliday, K.J., and Whitelam, G.C. (2003b). Phytochromes B, D, and E act redundantly to control multiple physiological responses in Arabidopsis. Plant Physiol. **131:** 1340–1346.

Goosey, L., Palecanda, L., and Sharrock, R.A. (1997). Differential patterns of expression of the Arabidopsis *PHYB*, *PHYD*, and *PHYE* phytochrome genes. Plant Physiol. **115:** 959–969.

Halliday, K.J., Salter, M.G., Thingnaes, E., and Whitelam, G.C. (2003). Phytochrome control of flowering is temperature sensitive and correlates with expression of the floral integrator FT. Plant J. **33:** 875–885.

Halliday, K.J., and Whitelam, G.C. (2003). Changes in photoperiod or temperature alter the functional relationships between phytochromes and reveal roles for phyD and phyE. Plant Physiol. **131:** 1913–1920.

Hirschfeld, M., Tepperman, J.M., Clack, T., Quail, P.H., and Sharrock, R.A. (1998). Coordination of phytochrome levels in phyB mutants of Arabidopsis as revealed by apoprotein-specific monoclonal antibodies. Genetics **149:** 523–535.

Huq, E., and Quail, P.H. (2002). PIF4, a phytochrome-interacting bHLH factor, functions as a negative regulator of phytochrome B signaling in Arabidopsis. EMBO J. **21:** 2441–2450.

Jones, A.M., and Quail, P.H. (1986). Quaternary structure of 124 kilodalton phytochrome from *Avena sativa.* Biochemistry **25:** 2987–2995.

Kevei, E., Schafer, E., and Nagy, F. (2007). Light-regulated nucleocytoplasmic partitioning of phytochromes. J. Exp. Bot. **58:** 3113–3124.

Khanna, R., Huq, E., Kikis, E.A., Al-Sady, B., Lanzatella, C., and Quail, P.H. (2004). A novel molecular recognition motif necessary for targeting photoactivated phytochrome signaling to specific basic helix-loop-helix transcription factors. Plant Cell **16:** 3033–3044.

Kim, J., Yi, H., Choi, G., Shin, B., Song, P.S., and Choi, G. (2003). Functional characterization of phytochrome interacting factor 3 in phytochrome-mediated light signal transduction. Plant Cell **15:** 2399–2407.

Kim, J.I., Bhoo, S.H., Han, Y.J., Zarate, X., Furuya, M., and Song, P.S. (2006). The PAS2 domain is required for dimerization of phytochrome A. J. Photochem. Photobiol. **178:** 115–121.

Kircher, S., Gil, P., Kozma-Bognar, L., Fejes, E., Speth, V., Husselstein-Muller, T., Bauer, D., Adam, E., Schäfer, E., and Nagy, F. (2002). Nucleocytoplasmic partitioning of the plant photoreceptors phytochrome A, B, C, D, and E is regulated differentially by light and exhibits a diurnal rhythm. Plant Cell **14:** 1541–1555.

Leivar, P., Monte, E., Al-Sady, B., Carle, C., Storer, A., Alonso, J.M., Ecker, J.R., and Quail, P.H. (2008). The *Arabidopsis* phytochrome-interacting factor PIF7, together with PIF3 and PIF4, regulates responses to prolonged red light by modulating phyB levels. Plant Cell **20:** 337–352.

Lorrain, S., Allen, T., Duek, P.D., Whitelam, G.C., and Fankhauser, C. (2008). Phytochrome-mediated inhibition of shade avoidance involves degradation of growth-promoting bHLH transcription factors. Plant J. **53:** 312–323.

Mathews, S. (2006). Phytochrome-mediated development in land plants: Red light sensing evolves to meet the challenges of changing light environments. Mol. Ecol. **15:** 3483–3503.

Mathews, S., and McBreen, K. (2008). Phylogenetic relationships of B-related phytochromes in the Brassicaceae: Redundancy and the persistence of phytochrome D. Mol. Phylogenet. Evol. **49:** 411–423.

Mathews, S., and Sharrock, R.A. (1997). Phytochrome gene diversity. Plant Cell Environ. **20:** 666–671.

Monte, E., Alonso, J.M., Ecker, J.R., Zhang, Y., Li, X., Young, J., Austin-Phillips, S., and Quail, P.H. (2003). Isolation and characterization

of *phyC* mutants in Arabidopsis reveals complex crosstalk between phytochrome signaling pathways. Plant Cell **15:** 1962–1980.

Monte, E., Tepperman, J.M., Al-Sady, B., Kaczorowski, K.A., Alonso, J.M., Ecker, J.R., Li, X., Zhang, Y., and Quail, P.H. (2004). The phytochrome-interacting transcription factor, PIF3, acts early, selectively, and positively in light-induced chloroplast development. Proc. Natl. Acad. Sci. USA **101:** 16091–16098.

Nagatani, A. (2004). Light-regulated nuclear localization of phytochromes. Curr. Opin. Plant Biol. **7:** 708–711.

Ni, M., Tepperman, J.M., and Quail, P.H. (1998). PIF3, a phytochrome-interacting factor necessary for normal photoinduced signal transduction, is a novel basic helix-loop-helix protein. Cell **95:** 657–667.

Ni, M., Tepperman, J.M., and Quail, P.H. (1999). Binding of phytochrome B to its nuclear signalling partner PIF3 is reversibly induced by light. Nature **400:** 781–784.

Oh, E., Kim, J., Park, E., Kim, J.I., Kang, C., and Choi, G. (2004). PIL5, a phytochrome-interacting basic helix-loop-helix protein, is a key negative regulator of seed germination in *Arabidopsis thaliana.* Plant Cell **16:** 3045–3058.

Park, E., Kim, J., Lee, Y., Shin, J., Oh, E., Chung, W.I., Liu, J.R., and Choi, G. (2004). Degradation of phytochrome interacting factor 3 in phytochrome-mediated light signaling. Plant Cell Physiol. **45:** 968–975.

Qin, M., Kuhn, R., Moran, S., and Quail, P.H. (1997). Overexpressed phytochrome C has similar photosensory specificity to phytochrome B but a distinctive capacity to enhance primary leaf expansion. Plant J. **12:** 1163–1172.

Quail, P.H. (2007). Phytochome-interacting factors. In Light and Plant Development, G.C. Whitelam and K.J. Halliday, eds (Oxford, UK: Blackwell Publishing), pp. 81–105.

Reed, J.W., Nagpal, P., Poole, D.S., Furuya, M., and Chory, J. (1993). Mutations in the gene for the red/far-red light receptor phytochrome B alter cell elongation and physiological responses throughout Arabidopsis development. Plant Cell **5:** 147–157.

Rockwell, N.C., Su, Y.S., and Lagarias, J.C. (2006). Phytochrome structure and signaling mechanisms. Annu. Rev. Plant Biol. **57:** 837–858.

Sharrock, R.A. (2008). The phytochrome red/far-red photoreceptor superfamily. Genome Biol. **9:** 230.

Sharrock, R.A., and Clack, T. (2002). Patterns of expression and normalized levels of the five Arabidopsis phytochromes. Plant Physiol. **130:** 442–456.

Sharrock, R.A., and Clack, T. (2004). Heterodimerization of type II phytochromes in *Arabidopsis.* Proc. Natl. Acad. Sci. USA **101:** 11500–11505.

Sharrock, R.A., Clack, T., and Goosey, L. (2003a). Signaling activities among the Arabidopsis phyB/D/E-type phytochromes: A major role for the central region of the apoprotein. Plant J. **34:** 317–326.

Sharrock, R.A., Clack, T., and Goosey, L. (2003b). Differential activities of the Arabidopsis phyB/D/E phytochromes in complementing *phyB* mutant phenotypes. Plant Mol. Biol. **52:** 135–142.

Sharrock, R.A., and Quail, P.H. (1989). Novel phytochrome sequences in *Arabidopsis thaliana*: Structure, evolution, and differential expression of a plant regulatory photoreceptor family. Genes Dev. **3:** 1745–1757.

Shen, H., Zhu, L., Castillon, A., Majee, M., Downie, B., and Huq, E. (2008). Light-induced phosphorylation and degradation of the negative regulator PHYTOCHROME-INTERACTING FACTOR1 from *Arabidopsis* depend upon its direct physical interactions with photoactivated phytochromes. Plant Cell **20:** 1586–1602.

Shen, Y., Khanna, R., Carle, C.M., and Quail, P.H. (2007). Phytochrome induces rapid PIF5 phosphorylation and degradation in response to red-light activation. Plant Physiol. **145:** 1043–1051.

Somers, D.E., Sharrock, R.A., Tepperman, J.M., and Quail, P.H. (1991). The *hy3* long hypocotyl mutant of *Arabidopsis* is deficient in phytochrome B. Plant Cell **3:** 1263–1274.

Takano, M., Inagaki, N., Xie, X., Yuzurihara, N., Hihara, F., Ishizuka, T., Yano, M., Nishimura, M., Miyao, A., Hirochika, H., and Shinomura, T. (2005). Distinct and cooperative functions of phytochromes A, B, and C in the control of deetiolation and flowering in rice. Plant Cell **17:** 3311–3325.

Terry, M.J., Maines, M.D., and Lagarias, J.C. (1993). Inactivation of phytochrome- and phycobiliprotein-chromophore precursors by rat liver biliverdin reductase. J. Biol. Chem. **268:** 26099–26106.

Wagner, J.R., Brunzelle, J.S., Forest, K.T., and Vierstra, R.D. (2005). A light-sensing knot revealed by the structure of the chromophore-binding domain of phytochrome. Nature **438:** 325–331.

Wagner, D., Koloszvari, M., and Quail, P.H. (1996). Two small spatially distinct regions of phytochrome B are required for efficient signaling rates. Plant Cell **8:** 859–871.

Wagner, J.R., Zhang, J., Brunzelle, J.S., Vierstra, R.D., and Forest, K.T. (2007). High resolution structure of *Deinococcus* bacteriophytochrome yields new insights into phytochrome architecture and evolution. J. Biol. Chem. **282:** 12298–12309.

Weller, J.L., Nagatani, A., Kendrick, R.E., Murfet, I.C., and Reid, J.B. (1995). New *lv* mutants of pea are deficient in phytochrome B. Plant Physiol. **108:** 525–532.

Yang, X., Kuk, J., and Moffat, K. (2008). Crystal structure of *Pseudomonas aeruginosa* bacteriophytochrome: photoconversion and signal transduction. Proc. Natl. Acad. Sci. USA **105:** 14715–14720.

Yang, X., Stojkovic, E.A., Kuk, J., and Moffat, K. (2007). Crystal structure of the chromophore binding domain of an unusual bacteriophytochrome, RpBphP3, reveals residues that modulate photoconversion. Proc. Natl. Acad. Sci. USA **104:** 12571–12576.

Zhu, Y., Tepperman, J.M., Fairchild, C.D., and Quail, P.H. (2000). Phytochrome B binds with greater apparent affinity than phytochrome A to the basic helix-loop-helix factor PIF3 in a reaction requiring the PAS domain of PIF3. Proc. Natl. Acad. Sci. USA **97:** 13419–13424.